

XMM-Newton Calibration Status Update

Michael Smith, ESAC

14th IACHEC, Shonan Village Center, 20-23 May 2019

1. Recent calibration file releases

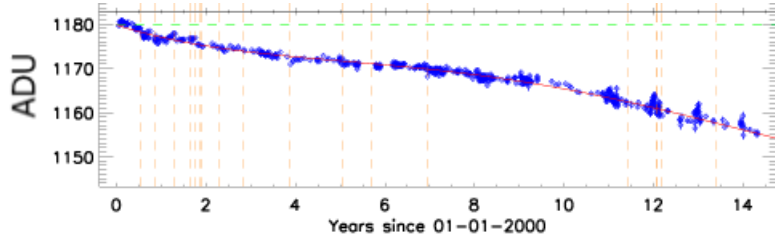
| | XMM-CCF-REL- |
|--|--------------|
| •OM photometry: update of time-dependent sensitivity degradation | 356 |
| •EPIC-pn energy scale: | |
| ○ Long-term CTI and quiescent background gain correction | 358 |
| ○ Long-term CTI for Small Window and Large Window modes | 366 & 367 |
| ○ Rate and energy dependent PHA correction for Timing Mode | 369 |
| •Astrometry: time variable boresight update | 361 |
| •EPIC-MOS energy scale: update of gain and CTI | 363 & 364 |

2. On-going calibration topics

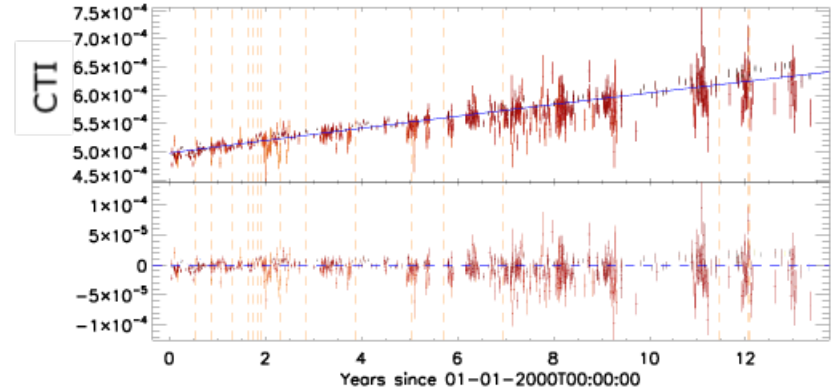
PN: Quiescent Background Gain Correction



“Empirical” method: derive LTCTI correction from polynomial fit to non-LTCTI corrected energies

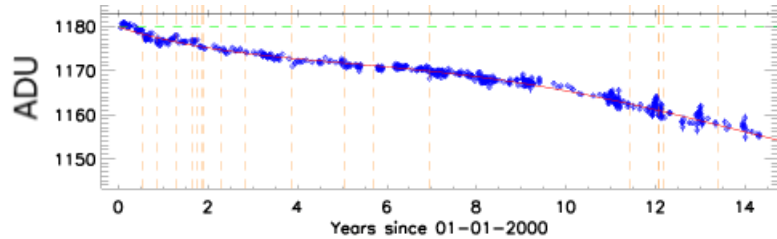


QBGC: (1) fit to measured CTI -> LTCTI correction

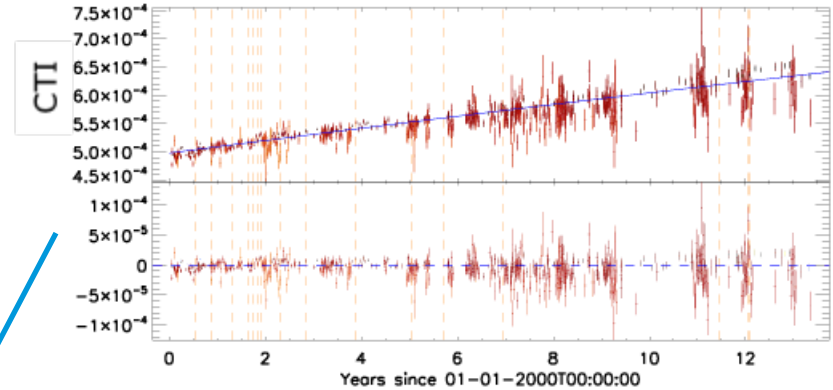


PN: Quiescent Background Gain Correction

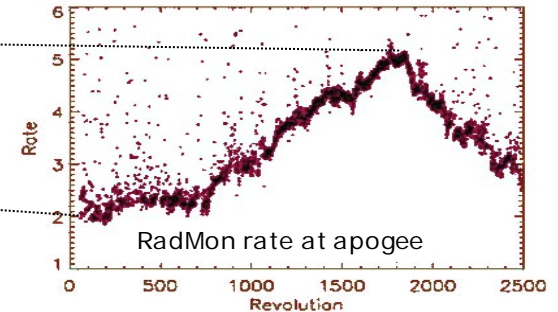
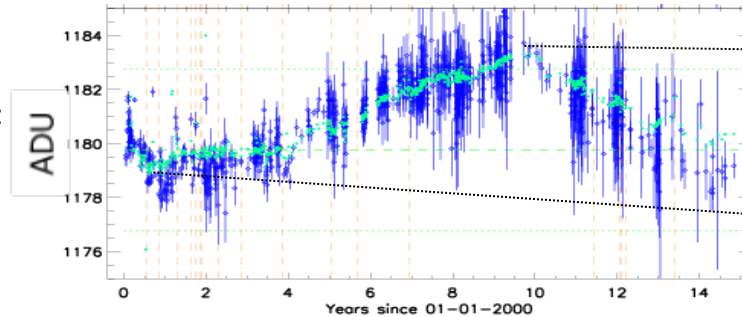
“Empirical” method: derive LTCTI correction from polynomial fit to non-LTCTI corrected energies



QBGC: (1) fit to measured CTI -> LTCTI correction



QBGC (2): residuals are due to QB dependent gain component; correct using NDISLIN(t) as proxy for QB



PN: Quiescent Background Gain Correction



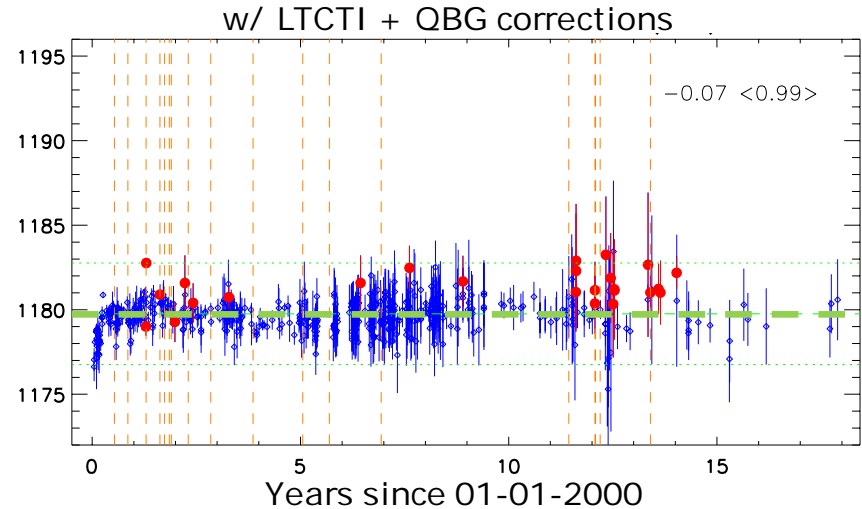
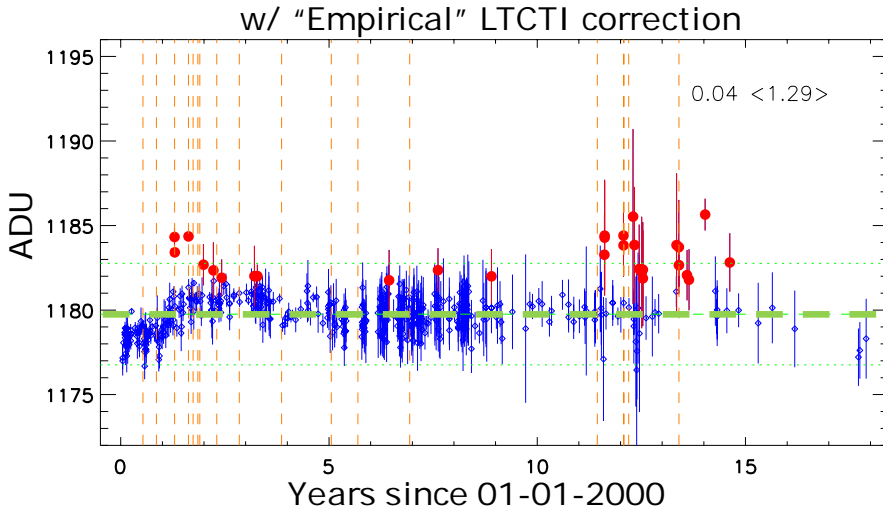
- Dependency of the EPIC-pn energy scale on the quiescent particle background rate: quiescent background-dependent gain (QBG)
- Time-dependent QBG correction implemented in SAS 17 (June 2018)
- QBG correction decoupled from the long-term CTI correction → XMM-CCF-REL-358 (Oct 2018). Calibrated for FF and EFF modes.



PN: Quiescent Background Gain Correction

- Dependency of the EPIC-pn energy scale on the quiescent particle background rate: quiescent background-dependent gain (QBG)
- Time-dependent QBG correction implemented in SAS 17 (June 2018)
- QBG correction decoupled from the long-term CTI correction → XMM-CCF-REL-358 (Oct 2018). Calibrated for FF and EFF modes.

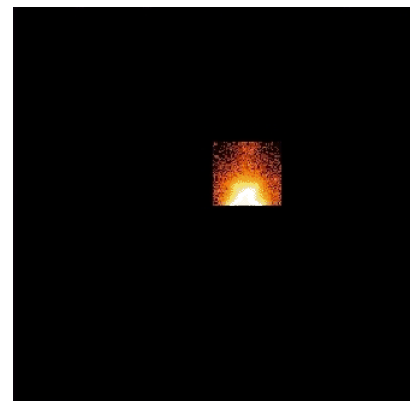
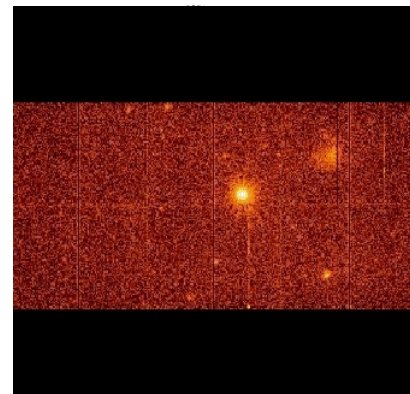
Energy reconstruction at Mn-Ka for the boresight:



PN: Energy Scale for Window Modes

PN Large and Small Window Modes long-term CTI correction:

- Derivation more problematic than for Full Frame Mode
- Very sparse sample of CalClosed exposures in window modes
- Use other data to derive LTCTI behaviour:
 - Fe-Ka emission from AGN
 - Cu-Ka fluorescence
 - Calibration released: XMM-CCF-REL-366 & 367 (2019)



➤ See Ivan Valtchanov's presentation in Detectors & Background working group

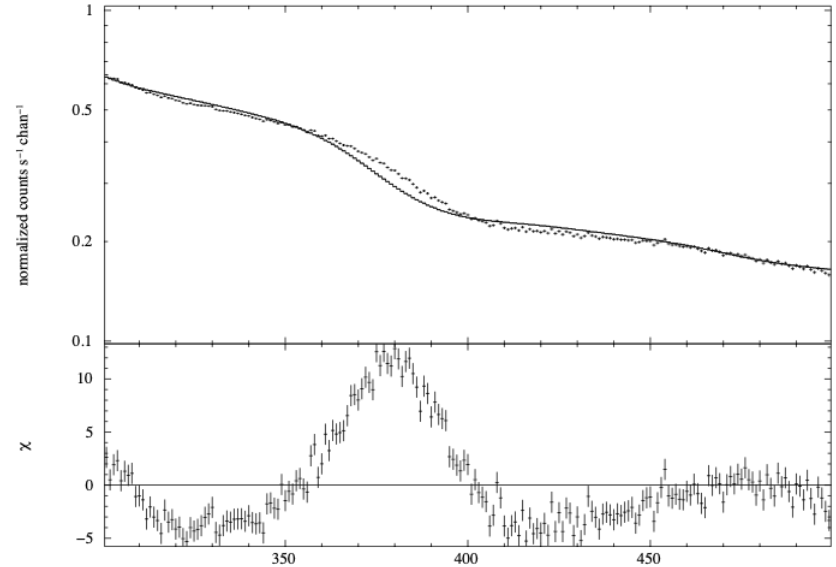
PN: Rate & Energy Dependent PHA Correction

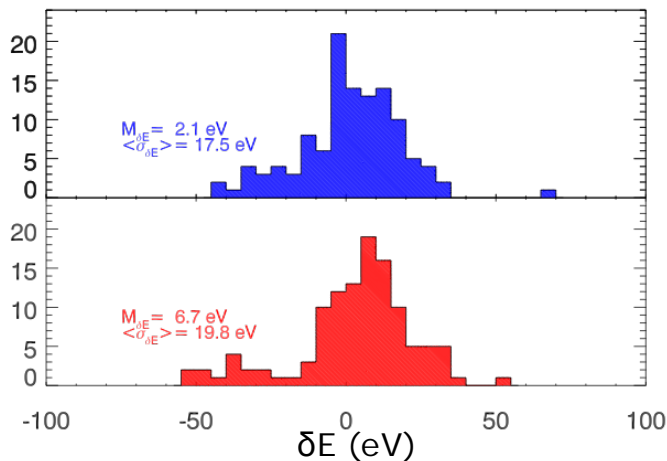
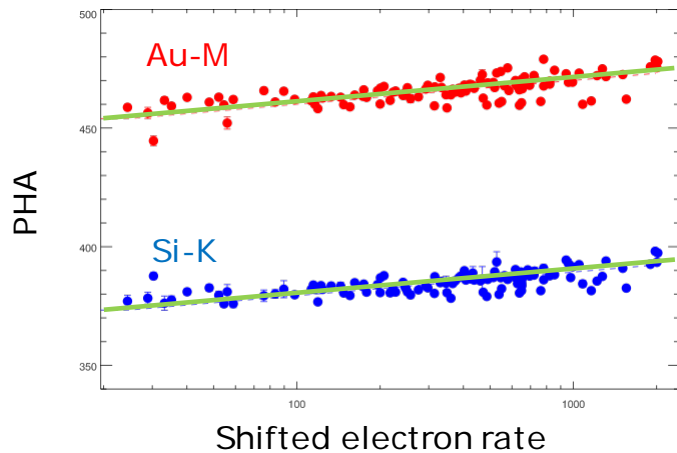


Calibration update to the rate-dependent PHA correction for PN Timing Mode

This new correction builds on that of Guainazzi et al. (2013, 2014):

- Derived from a significantly larger sample (~ 150 sources)
- In addition to the instrumental edges at Si-K (1.8 keV) and Au-M (2.2 keV) now includes high energy data point at Au-L (11.9 keV)
- Details in XMM-CCF-REL-369 (Migliari et al. 2019)

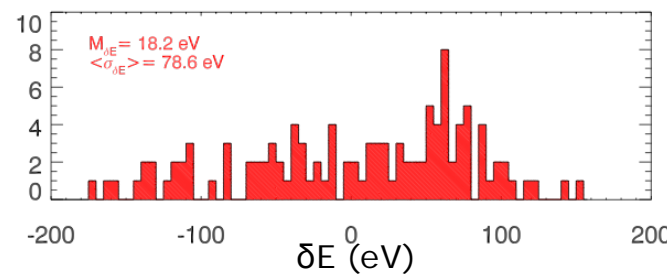
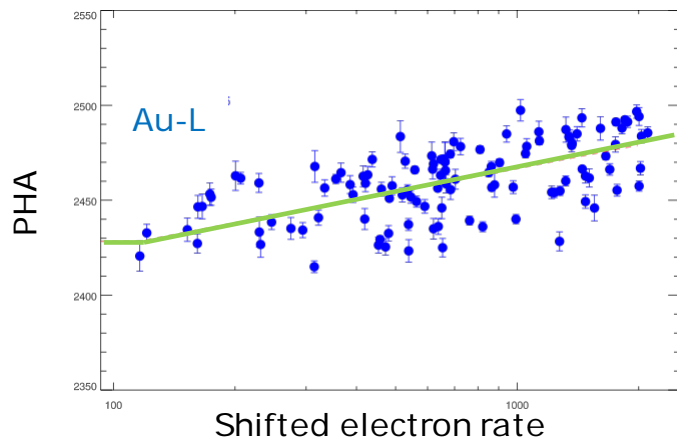




at ~2 keV:

average systematics
~1%

tail to 70 eV (3.5%)



at ~12 keV:

average systematics
~0.7%

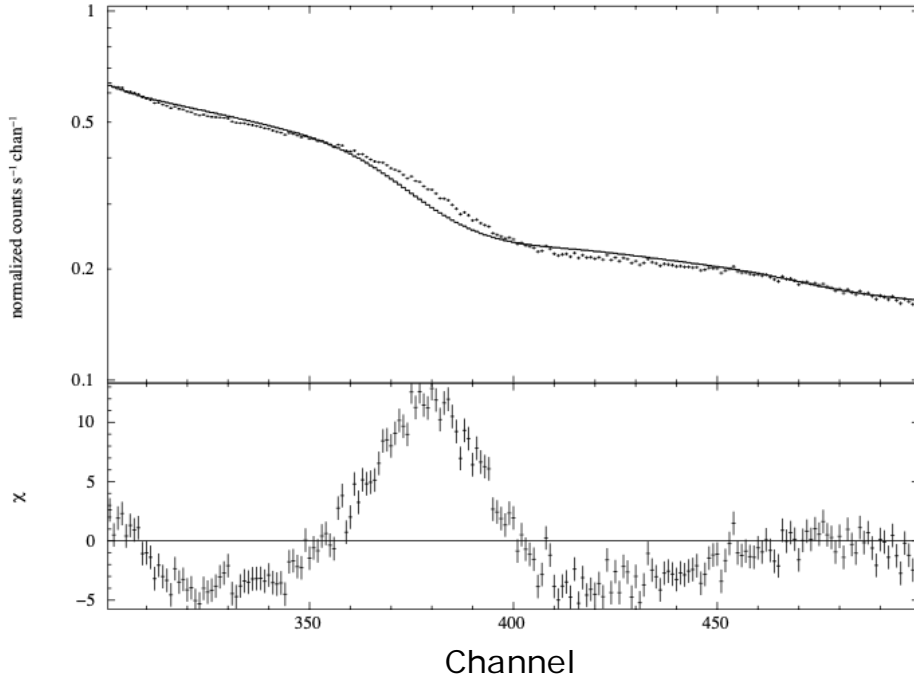
tail to 180 eV (1.5%)

S. Migliari

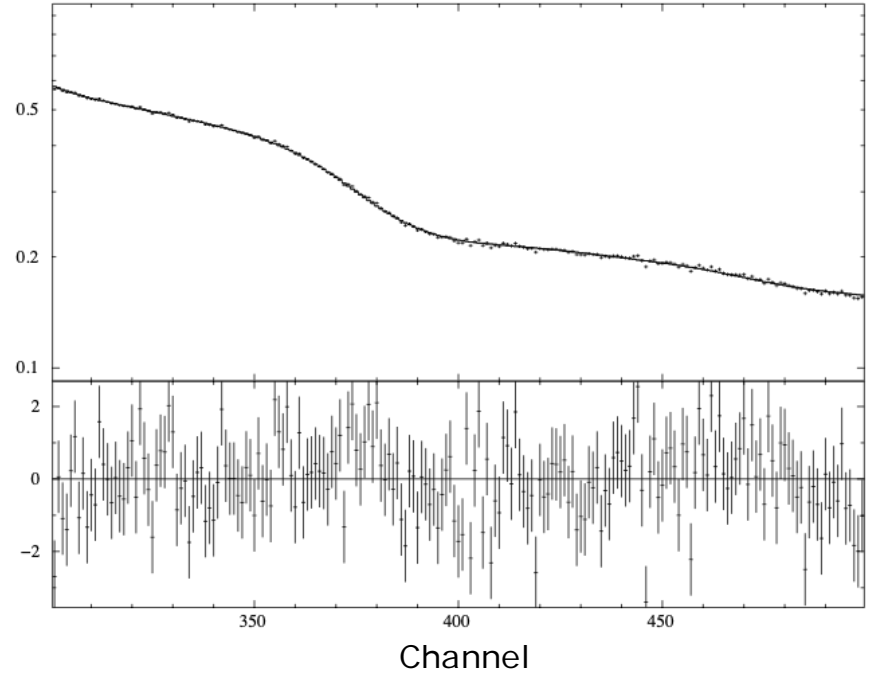
PN: Rate & Energy Dependent PHA Correction



No RDPHA correction



With RDPHA correction



S. Migliari



OM: Release of SUSS4.1



Release of the Serendipitous UV Source Survey v4.1 (the “OM Catalogue”):

- Version 4: SUSS4.1, released in December 2018 (available via XMM XSA)
- All public observations up to July 2017
- Full reprocessing with SAS 17:
- 8.18×10^6 detections of 5.5×10^6 unique sources, from 9749 XMM-Newton pointings
- 4.45×10^6 detections with UV data (3.05×10^6 unique sources)
- Source variability from multiple pointings (1.04×10^6 sources observed > once)
- 82% of cleanest, point-like OM sources have a match in GAIA DR2 catalogue
 - 98% of those are within 2", median offset 0.45"



1. Recent calibration file releases

| | XMM-CCF-REL- |
|--|--------------|
| •OM photometry: update of time-dependent sensitivity degradation | 356 |
| •EPIC-pn energy scale: | |
| ○ Long-term CTI and quiescent background gain correction | 358 |
| ○ Long-term CTI for Small Window and Large Window modes | 366 & 367 |
| ○ Rate and energy dependent PHA correction for Timing Mode | 369 |
| •Astrometry: time variable boresight update | 361 |
| •EPIC-MOS energy scale: update of gain and CTI | 363 & 364 |

2. On-going calibration topics

OM: Grism t-Dependent Sensitivity Correction



OM is subject to time-dependent sensitivity degradation

A correction for visible + UV filter data implemented in 2006

Correction for V and UV grism data will be released soon:

OM_GRISMAL_0005.CCF

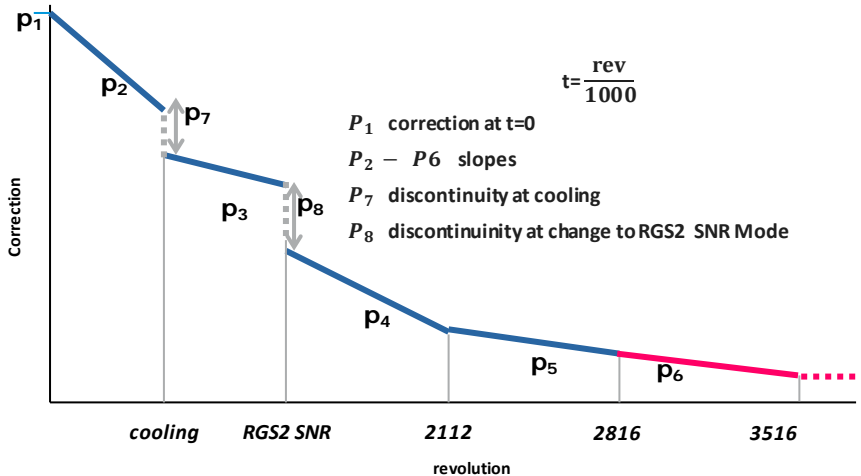
(with SAS 18)

| Year | UV_Grism | V_Grism |
|------|----------|---------|
| 2000 | 1.00 | 1.00 |
| 2002 | 1.01 | 1.01 |
| 2004 | 1.02 | 1.02 |
| 2006 | 1.04 | 1.02 |
| 2008 | 1.05 | 1.03 |
| 2010 | 1.07 | 1.04 |
| 2012 | 1.08 | 1.04 |
| 2014 | 1.10 | 1.05 |
| 2016 | 1.12 | 1.06 |
| 2018 | 1.13 | 1.07 |
| 2020 | 1.15 | 1.07 |



RGS: A_{eff} Correction Update

- Evidence for a systematic change in time in the RGS1 to RGS2 flux ratios
- Corrected through epoch and energy dependent model (**RGSn_EFFAREACORR** CCFs)
- Updated correction with improved algorithm and validity range → to be released soon



For each 0.05 Å bin:

$$t < 0.538 \quad P_1 + \left(\frac{t}{0.538}\right) P_2$$

$$0.538 \leq t < 1.408 \quad P_1 + P_2 + P_6 + \left(\frac{t - 0.538}{0.870}\right) P_3$$

$$1.408 \leq t < 2.112 \quad P_1 + P_2 + P_3 + P_7 + P_8 + \left(\frac{t - 1.408}{0.704}\right) P_4$$

$$2.112 \leq t < 2.816 \quad P_1 + P_2 + P_3 + P_4 + P_7 + P_8 + \left(\frac{t - 2.112}{0.704}\right) P_5$$

$$2.816 \leq t < 3.516 \quad P_1 + P_2 + P_3 + P_4 + P_5 + P_7 + P_8 + \left(\frac{t - 2.816}{0.700}\right) P_6$$

+ narrow gaussians at specific wavelengths

J. Kaastra, C. de Vries & J.W. den Herder, 2019

RGS: Changing A_{eff}

Evidence for decreasing effective area

- Flux decrease observed in:

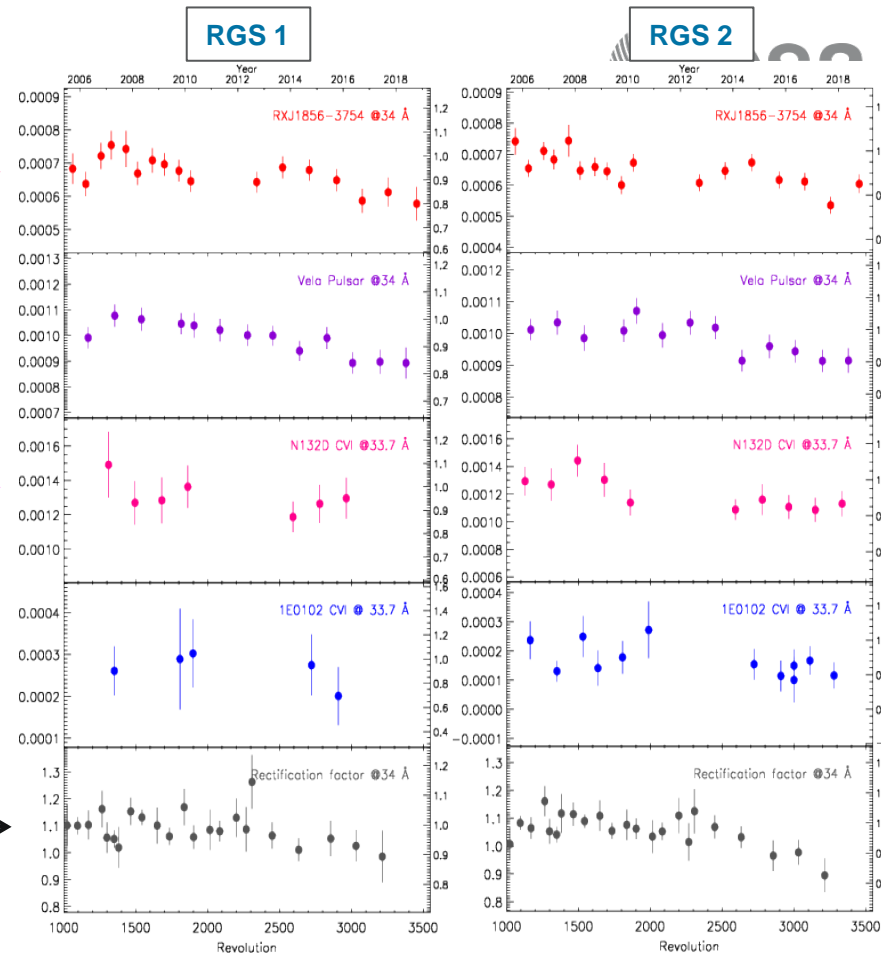
ISN RXJ1856-3754

Vela Pulsar

Emission lines in compact SNRs
N132D

1E0102

- Decrease of the ratio of fluxes RGS/EPIC-pn (aka "Rectification Factors")



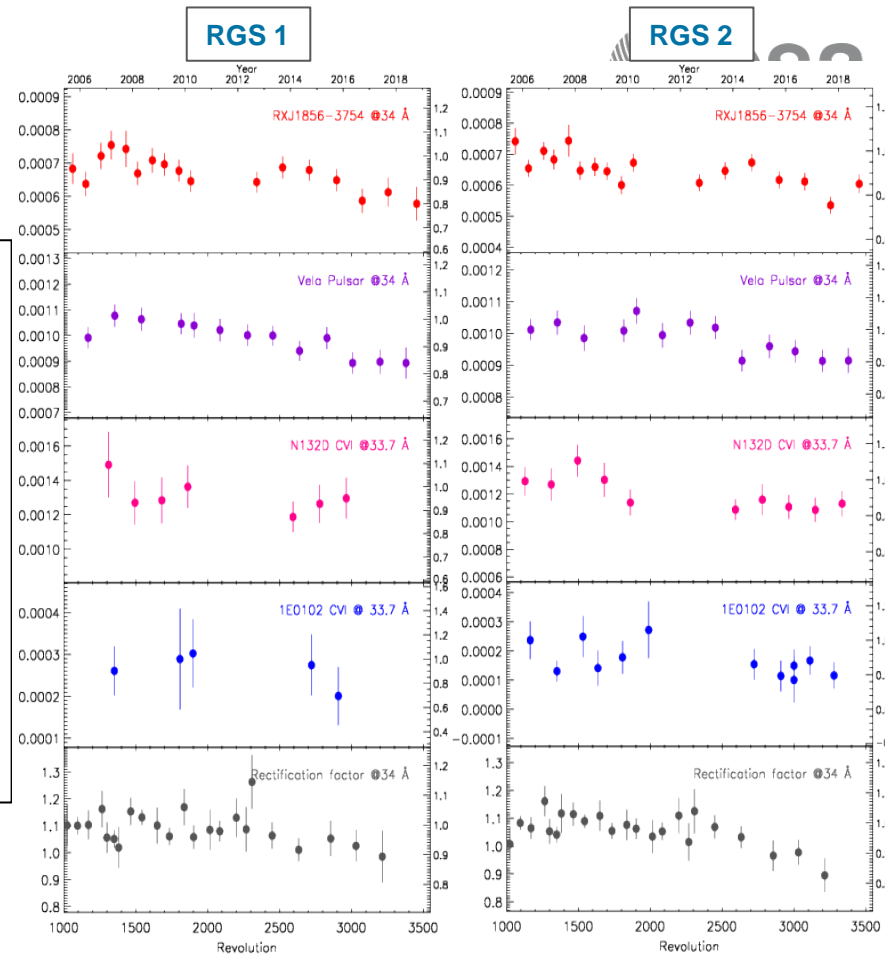
RGS: Changing A_{eff}

Evidence for decreasing effective area

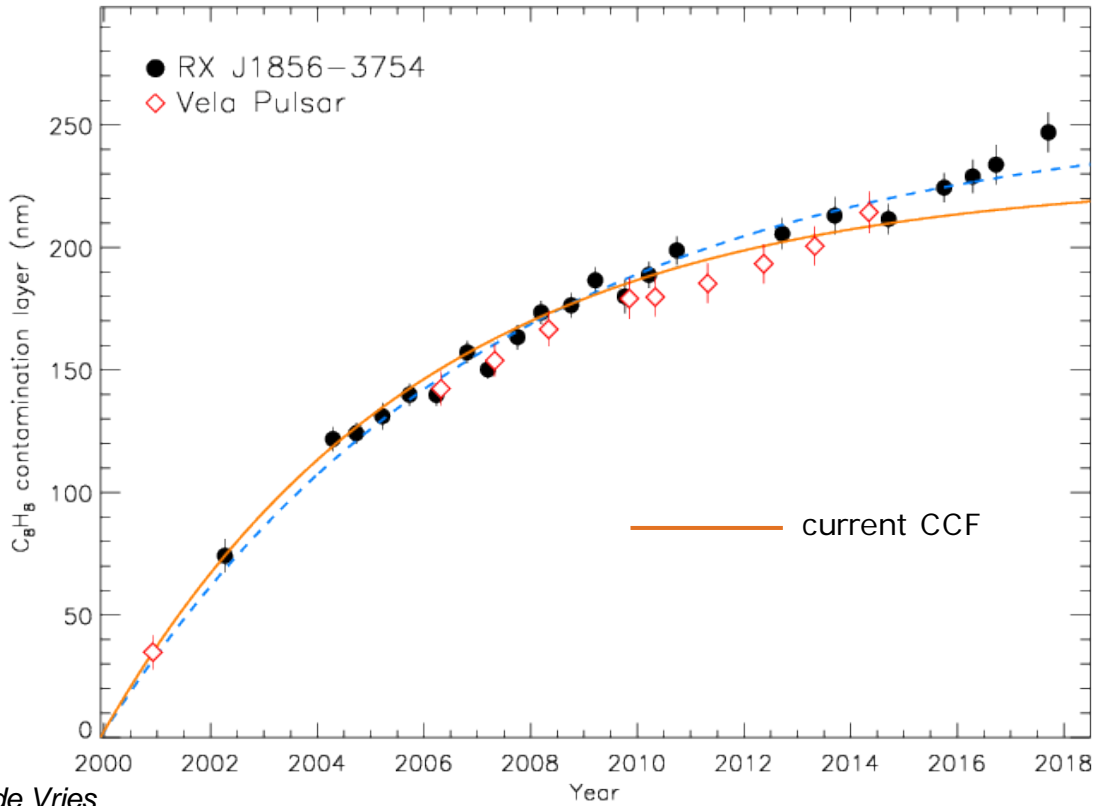
Possible instrumental causes:

- Increase in the thickness of the C_8H_8 contamination layer
✗ very different wavelength dependence
- Increase in the thickness of the O layer
✗ would require an increase of 300 nm
- Mismatch in the PI selection regions
✗ would imply an unrealistic error in gain

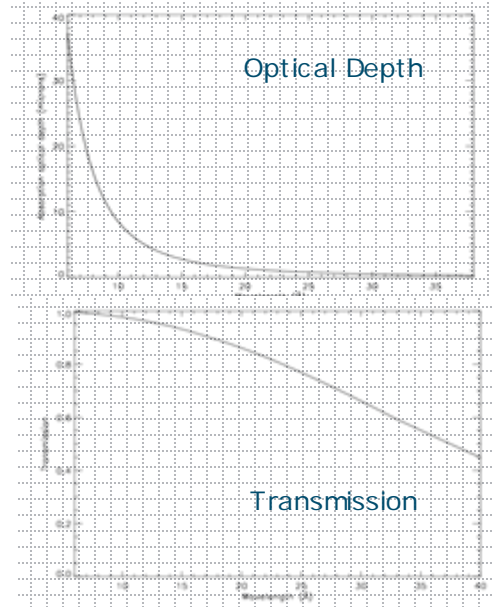
→ work in progress...



RGS: Contamination Monitoring



Thickness of layer \propto flux @35Å

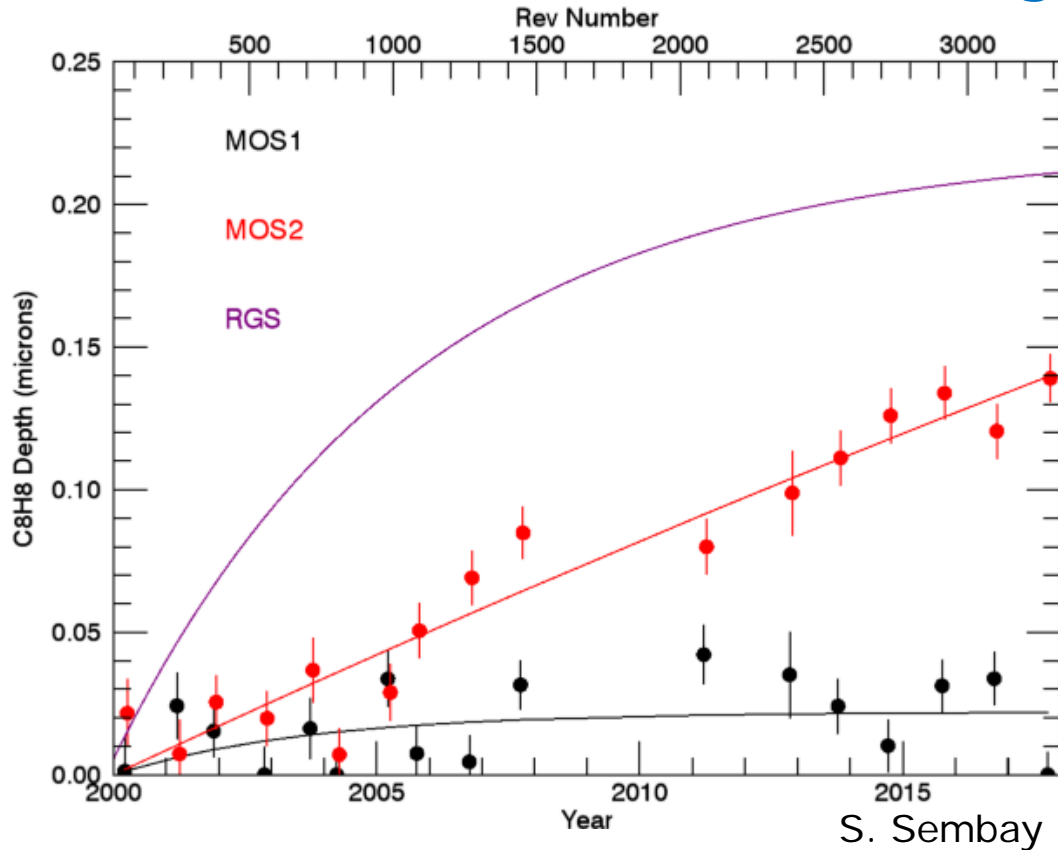


Indications of increasing contamination?

C. de Vries



MOS: Contamination Monitoring



Primary monitoring source:
SNR 1E0102.

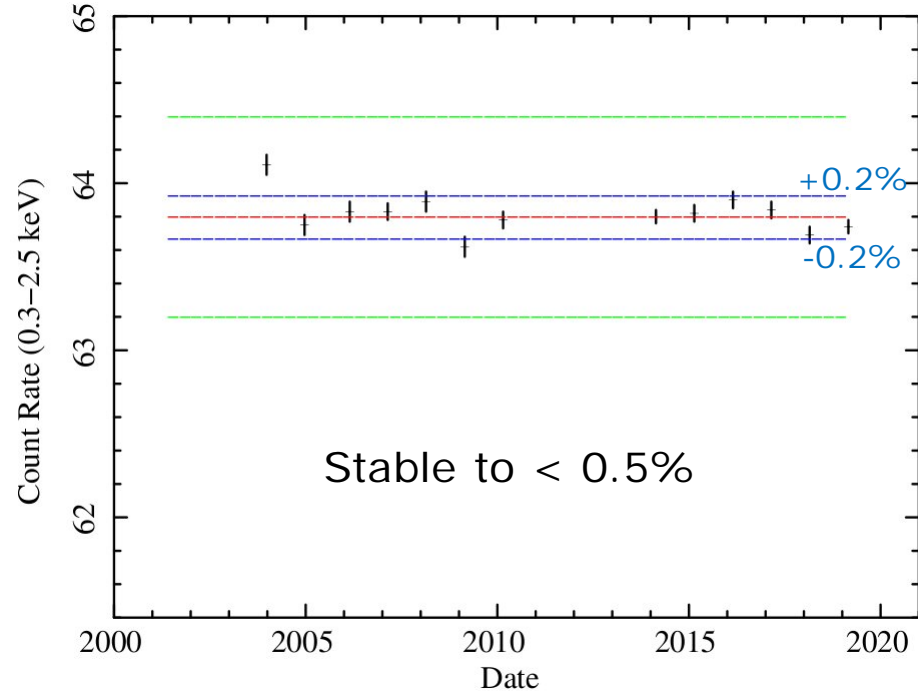
Contamination status in 2018 shows no
change in trend:

- MOS1 stable
- MOS2 steadily increasing:
~ 14% A_{eff} loss @ 0.5 keV in 2018

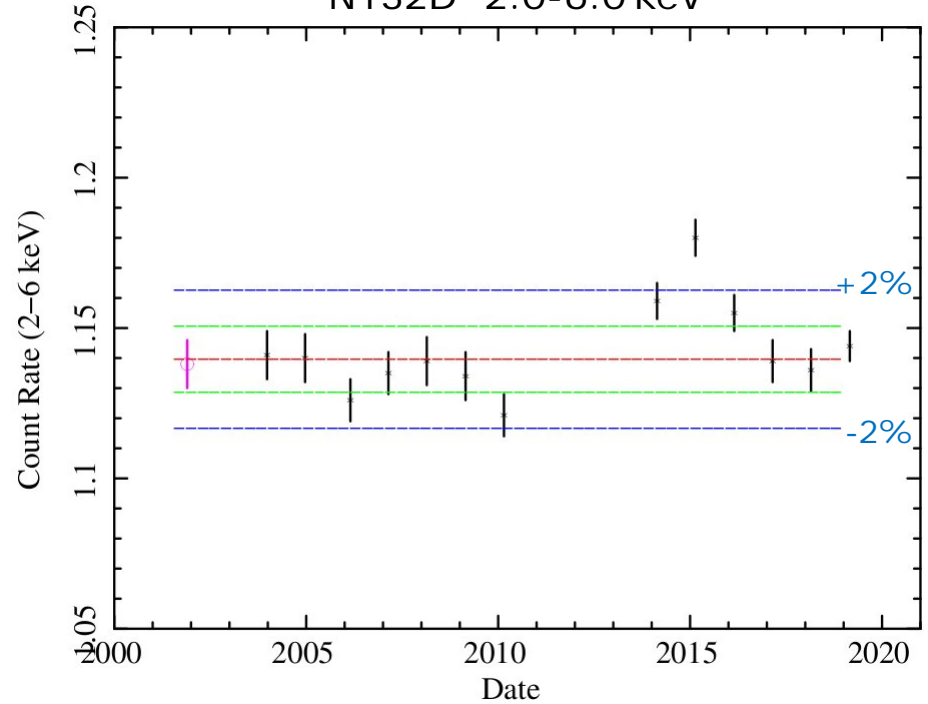
PN: Stability Monitoring



N132D 0.3-2.5 keV



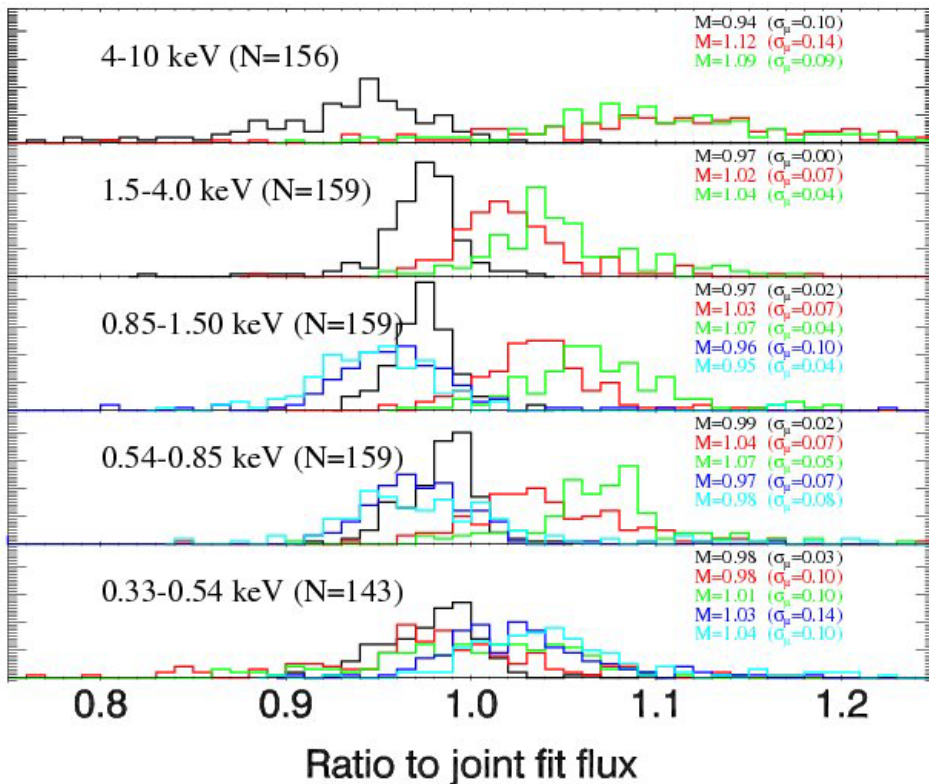
N132D 2.0-6.0 keV



Details in R. Saxton, 2019, XMM-SOC-CAL-TN-0212



Cross Calibration Status



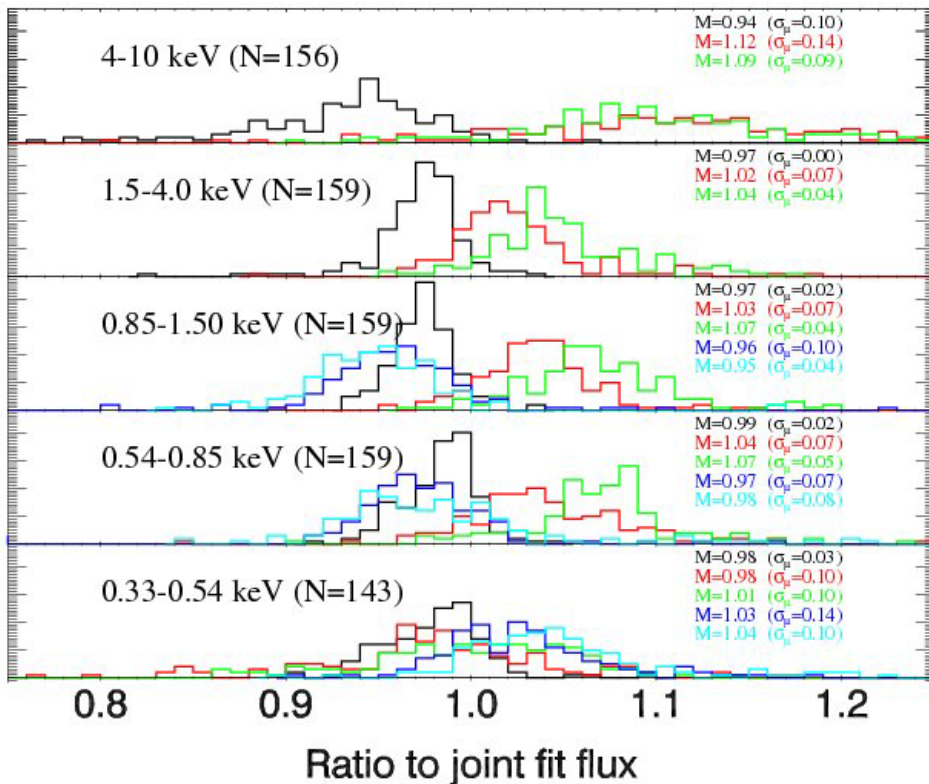
PN
MOS1
MOS2
RGS1
RGS2

Instrumental flux ratios derived from a set of ≈ 120 observations in the XMM-Newton Cross-Calibration Database.

- MOS1 / pn:
 - ≈ 1.00 ($E < 0.54$ keV)
 - ≈ 1.05 ($E > 0.54$ keV)
- MOS2 / pn:
 - ≈ 1.03 ($E < 0.54$ keV)
 - ≈ 1.08 ($E > 0.54$ keV)
- MOS / pn above > 4 keV: ≈ 1.1
- RGS / pn: From 1.05 to 0.98 with increasing E



Cross Calibration Status



PN
MOS1
MOS2
RGS1
RGS2

Instrumental flux ratios derived from a set of ≈ 120 observations in the XMM-Newton Cross-Calibration Database.

- MOS1 / pn:
 - ≈ 1.00 ($E < 0.54$ keV)
 - ≈ 1.05 ($E > 0.54$ keV)
- MOS2 / pn:
 - ≈ 1.03 ($E < 0.54$ keV)
 - ≈ 1.08 ($E > 0.54$ keV)
- MOS / pn above > 4 keV: ≈ 1.1
- RGS / pn: From 1.05 to 0.98 with increasing E

The CORRAREA MOS / pn correction is currently being recalibrated:

Applies an empirical A_{eff} correction to the EPICs.

➤ See talk by Christian Pommranz in Calibration Methods session.

